

# Application of frequency domain induction EM soundings with controlled source (FDEMS method) for precise tracing of boundaries in geoelectrical sections

**Igor Ingerov\***

Advanced Geophysical Operations  
and Services Inc. (AGCOS)  
162 Oakdale Road,  
Toronto, Ontario, M3N2S5  
Canada  
[ingerov@agcos.ca](mailto:ingerov@agcos.ca)

**Andrii Lozoviy**

National Mining University  
of Ukraine (NGU)  
pr. Dmytra Yavornytskoho, 19,  
Dnipro, Dnipropetrovsk Oblast,  
Ukraine, 49600  
[lozovoy\\_dp.ua@ukr.net](mailto:lozovoy_dp.ua@ukr.net)

**Yana Mendrii**

National Mining University  
of Ukraine (NGU)  
pr. Dmytra Yavornytskoho, 19,  
Dnipro, Dnipropetrovsk Oblast,  
Ukraine, 49600  
[ianamendrii@gmail.com](mailto:ianamendrii@gmail.com)

## SUMMARY

The FDEMS method was introduced in the former USSR at the turn of the 50s and 60s of the last century as an integral part of the triad of induction EM methods (MT, FDEMS, TDEM), which were actively developed in the 50s after the grand discoveries by A.N. Tikhonov and L. Cagniard. The method was not widely used, primarily due to lack of suitable hardware and software for data processing and interpretation. Nevertheless, FDEMS was actively developed in certain regions of Russia and Ukraine until the present days. Interest in the method is supported by the potentially high accuracy of mapping high-resistivity boundaries, since in the FDEMS method there is a direct relationship between the ratio ( $R/H$ ) of the sounding spacing ( $R$ ) to the depth ( $H$ ) to the high-resistivity reference horizon pronounced by significant points of amplitude and phase frequency characteristics (curves). A number of successful FDEMS surveys were completed on the Ukrainian Shield and its slopes, Dnipro-Donetsk basin (Ukraine) and different parts of Russia and Uzbekistan which achieved positive results (1977-2000). To date, the capabilities of modern multifunction and multichannel equipment, software for processing and interpreting field data allows to realize to a large extent the prospective capabilities of the FDEMS method for high-precision mapping of boundaries in the geoelectric section and mapping of low-contrast objects.

**Key words:** induction electromagnetic sounding, control source, frequency domain, geoelectrical section, mining.

## INTRODUCTION

The FDEMS method appeared in the former USSR in the 50s of the last century as part of a group of three induction methods (MT, FDEMS, TDEM), which were based on the article published by Academic A.N. Tikhonov (Tikhonov, 1950, Cagniard, 1953). The method was predominantly developed in the Laboratory of Electromagnetic Studies of the Geological Institute of the USSR Academy of Sciences under the direction of B.S. Enenstein. By the early sixties, three variants of field equipment were developed: high-frequency (100,000 - 1000 Hz), mid-frequency (10,000 - 1 Hz) and low-frequency (500 - 0.01 Hz) together with methods for interpreting the significant points of curves and templates of theoretical curves (Enenstein, 1961, Enenstein et al., 1967, Ivanov, 1983, Shevnia, 1973, Ingerov and Soldatenko, 1998). The low-frequency version of the equipment was further developed in the well-known CES-1 (Ingerov, 2011) and ERES-67 equipment, which were successfully produced before the beginning of the 90s of the last century. The mid-frequency version of the equipment (NCHZ-64 and NCHZ-73) was also developed under the leadership of A.P. Ivanov (1983). Significant contributions to the development of the method were also made by Vanyan (1965), Kulikov and Shemyakin (1978). During the period from 1978 to 1994, the most active field surveys were carried out in Ukraine and Russia for hydrocarbon deposits exploration in the Dnipro-Donetsk basin (Ingerov et al, 1990) and mapping of the Ukrainian crystalline shield (Ingerov et al., 1990). At the present time, the emergence of wideband multichannel equipment opens up entirely new possibilities for the application of the FDEMS method as a high-precision solution for solving a wide range of geological problems (Ingerov et al., 2016, Lozovoy et al., 2011).

## THE CORE PARTICULARITIES OF THE FDEMS CURVES BEHAVIOUR OVER THE SECTIONS AND THE HIGH-RESISTIVITY REFERENCE HORIZON

For the frequency domain EM soundings, the artificial electromagnetic field is created either by horizontal electric ( $P_x$ ) or vertical magnetic ( $M_z$ ) dipoles. The  $P$  is a galvanic electrical line AB,  $M$  - induction loop Q. The intensity of the created field is determined by the dipole moments:

$$P_x = |AB| \cdot I; M_z = \mu \cdot Q \cdot I \quad (1)$$

where,  $I$  - the current in the AB dipole or the loop Q,  $AB$  - the length of the electric dipole,  $Q$  - the effective area of the magnetic dipole, and  $\mu$  - the relative magnetic permeability.

At some distance  $R$  between the centres of the power and receiving dipoles, which is called the spacing of the electroprospecting array, one or several components of the electromagnetic field are measured, for example, horizontal electric  $E_x$  parallel to the source dipole AB and vertical magnetic  $H_z$ . In practice, axial (AB<sub>1</sub>-MN<sub>1</sub>) or equatorial (AB<sub>2</sub>-MN<sub>2</sub>) arrays are most often used (Figure 1).

The amplitude of electromagnetic field at the measurement site will be determined by the moment of the power dipole, the value of spacing ( $R$ ) between source of EM field and receiver, the sounding frequency ( $f$ ), and the geoelectrical section predominantly below the field measurement site. When the distance between receiver and control source is increased, i.e. the spacing of the array ( $R$ ) is changed, the principle of geometric sounding is realized, whereas the frequency of the source field ( $f$ ) remains constant. Thus, while keeping the spacing ( $R$ ) constant, but changing the frequency of the control source, the principle of induction sounding (skin effect) is realized. Therefore, the FDEMS soundings carried out at different spacing's with a sweep of different frequencies  $f_i$  ( $i = 1 \div n$ ), combine two types of soundings, geometric and inductive (substantially predominant) and, as a result, potentially have an increased resolution capabilities with respect to other electroprospecting methods.

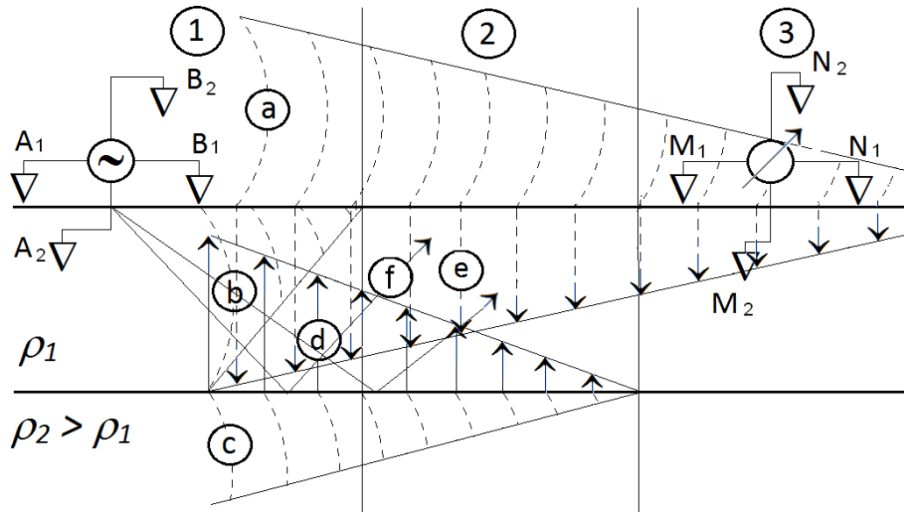


**Figure 1: Diagram of propagation of current source's electromagnetic waves over a horizontally-layered section with a high-resistivity basement; Dipole axial A<sub>1</sub>B<sub>1</sub>M<sub>1</sub>N<sub>1</sub> and equatorial A<sub>2</sub>B<sub>2</sub>M<sub>2</sub>N<sub>2</sub> electroprospecting field arrays.**

The main types of electromagnetic (EM) waves that participate in signal formation in the FDEMS method are shown in Figure 1. The numerals denote the near (1) intermediate (2) and far (3) zones of a harmonious EM field source. The index (a) denotes the wave propagating through the air, (e) - the induction of the first planar inhomogeneous wave (a) propagating in the earth, (c) - the refracted wave in the high-resistivity layer, (d) - the refracted wave in the low-resistivity layer, (b) - propagation from a source in a low-resistivity layer, (f) - wave reflected at the border of first low-resistivity and second high-resistivity horizon. The far zone (3) of the source has the same properties as in the MT soundings, similar to the CSAMT method, where the direct EM wave is inhomogeneous, and it decays with the increase of the distance from the source. In the near zone (1), the detected signal is determined by the summary characteristics of the medium, primarily its total conductivity  $S$ . The most interesting is the intermediate zone (2), where interference at the point of measurement of direct (a), reflected (f) and refracted (d) waves causes high sensitivity to changes in parameters of the geoelectrical section. By manipulating the spacing  $R$ , the system can be configured for the maximum EM response for a specific depth interval. Noteworthy, the borders of zones 1, 2 and 3 are not fixed and are very dependable on the frequency of the EM field. Therefore, they will be moving away from the source dipole with the decrease of the frequency.

### CHARACTERISTICS OF THE FDEMS CURVES FOR SECTIONS WITH PRESENCE OF HIGH-RESISTIVITY HORIZONS

The response functions of the medium in FDEMS are measured at certain distance  $R$  from the power source AB or the power loop  $Q$  at one or more sites to estimate the amplitude and phase of EM signal using galvanic measuring lines MN or induction loop  $q$  as well as induction coils (IC). In this case, the amplitude of apparent resistivity curve is constructed from amplitude measurements ( $\Delta U$ ) as a function of frequency:

$$\rho_{\omega} = k \frac{\Delta U_{MN(q)}}{I_{AB(Q)}} \quad (2)$$

where,  $k$  - the geometric coefficient of the field array;  $\Delta U$  - amplitude of the signal in the receiving line MN or receiving loop  $q$ ;  $I$  - the amplitude of current in the power dipole AB or power loop  $Q$ . The geometric coefficient for equatorial array is determined by the expressions for the components  $E_x$  and  $B_z$  respectively (Vanyan, 1965):

$$k_{E_x} = \frac{\pi R^3}{AB \cdot MN}; \quad k_{B_z} = \frac{2\pi R^4}{MN \cdot q} \quad (3)$$

The phase frequency response is defined as the phase shift between the signals ( $\varphi_{MN}$ ) at the measurement sites and the current at the control source ( $\varphi_{AB}$ ):

$$\varphi = \varphi_{MN(Q)} - \varphi_{AB(Q)} \quad (4)$$

Measurement of the absolute phase in the field conditions causes complications for hardware development, therefore, not the absolute phase which is determined by the equation above, but the differential phase parameter (Kulikov and Shemyakin, 1978) is used:

$$\Delta\varphi = \varphi - \omega \frac{\partial\varphi}{\partial\omega} \quad (5)$$

In practice, the finite difference differential parameter is used, which is a phase shift, for example, between the first and third harmonics of the signal at the measurement site (Kulikov and Shemyakin, 1978):

$$\Delta\varphi = \frac{\omega_3\varphi_1 - \omega_1\varphi_3}{\omega_3 - \omega_1} = \frac{3\varphi_1 - \varphi_3}{2} \quad (6)$$

The  $\Delta\varphi_{MN(Q)}$  value of measurement site is usually corrected by the value of  $\Delta\varphi_{AB(Q)}$  at the source dipole at each frequency. The FDEMS amplitude curves are plotted on the logarithmic scale. The  $\log \rho_\omega$  is plotted along the ordinates axis, whereas  $\log T$  is plotted along abscises axis, where  $T = l/f$  is the period of the wave. Phase curves ( $\varphi$  or  $\Delta\varphi$ ) are plotted on a semi-logarithmic scale. On the ordinates axis plotted is  $\varphi$  ( $\Delta\varphi$ ) on a linear scale with the sign taken into account, whereas  $\log T$  is plotted along the abscissa axis on logarithmic scale (Figure 2). The shape and amplitude of the curves depends on the nature of the geoelectrical section and the soundings spacing ( $R$ ), as well as the selected frequency interval. Since the FDEMS method combines geometric (the dependence of the penetration depth of the electromagnetic field on the spacing ( $R$ )) and induction (the dependence of the field penetration depth from its period  $T$ ) principles, it is possible to optimize the response of the medium for the depth interval of interest by manipulating the spacing and frequency of the EM field. The high resolution capability of the FDEMS method for sections with a high resistivity reference horizon is facilitated by the presence of deep interference extrema associated with interference of direct, reflected and refracted waves in the intermediate zone of the control source (Figure 1, 2). Figure 2 shows FDEMS amplitude and phase curves  $\Delta\varphi$  (in the frequency range from 10,000 to 0.1 Hz) for a two-layer section with the following parameters:  $\rho_1 = 10$  Ohm,  $\rho_2 = 1000$  Ohm,  $h_1 = 100$  m,  $S_l = 100 / 10 = 10$ Sm, sounding spacing  $R = 300$  m;  $R/h_1 = 3$ .

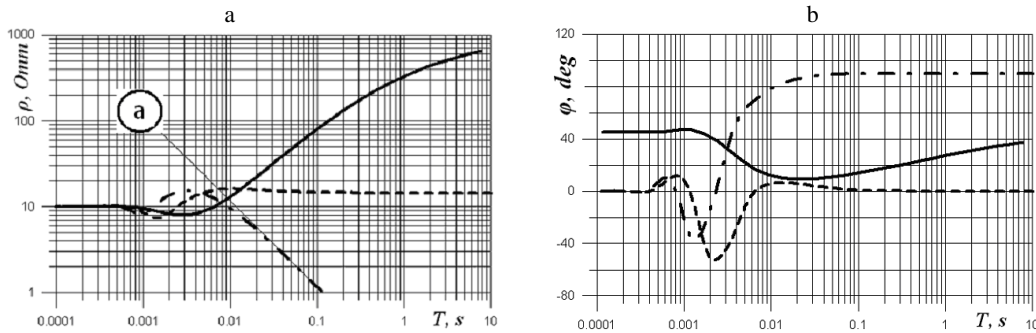


**Figure 2: The FDEMS and AMT amplitude (a) and phase (b) curves above two-layer section. Solid lines - AMT curves, dotted lines- FDEMS  $E_x$  curves, Bar-dotted lines - FDEMS  $B_z$  curves.**

The curves are given for parallel electric  $E_x$  and vertical magnetic  $B_z$  ( $\frac{\partial B_z}{\partial\omega}$ ) components of the electromagnetic field in the equatorial region of the control source. The same figure shows the amplitude and phase (differential phase parameter  $\Delta\varphi$ ) curves for the AMT method, which characterize the behaviour of the response functions of the medium for a plane homogeneous electromagnetic wave (Ingerov et al., 2012, 2015). A horizontal (left) asymptote is observed on the amplitude curves in the high-frequency region, passing at the level of the resistivity of the first layer, i.e. 10 Ohm. For the FDEMS phase curves, the left horizontal asymptote passes at  $0^\circ$  level, in contrast to the AMT method, in where it passes at  $45^\circ$  level. It should be noted, that the amplitude curves for FDEMS and AMT in the region of the left asymptote and somewhat to the right completely coincide, whereas the phase curves are similar in shape, but differ by  $45^\circ$ . Further, as the frequency is lowered, the low-visibility minimum is observed on the FDEMS amplitude curves, then the maxima of the larger amplitude is followed, and finally, the steep descending branch leading to the acute minima. On the phase curves, the marked elements look much clearer. Starting with the falling branch, the amplitude curves of FDEMS and AMT begin to diverge substantially. At the same time, the FDEMS electrical component has relatively sharp minima, an ascending branch, a very flat maxima, and a transfer to the right horizontal asymptote, while the minima of AMT is flat and wide, whereas the abscissa  $T_{min}$  of the AMT curves minima is situated at the significantly lower frequency (Figure 2). A remarkable fact is the relation between the value of  $\rho_a$  on the right asymptote and the total longitudinal conductivity in siemens which is determined by the equation:

$$S_1 = \frac{R}{2 \cdot \rho_a} \quad (7)$$

where,  $\rho_a$  - the apparent resistivity value on the right asymptote;  $R$  - sounding spacing.

In our particular case,  $\rho_a = 15 \text{ Ohm}$ . The AMT amplitude curve in this case extends the ascending branch to the resistivity level of the second layer, i.e. up to 1000 Ohm. The angle of inclination of this curve is close to  $45^\circ$ . The FDEMS phase curves have rather sharp minima. These minima are much deeper than the minima on the AMT phase curves. After the ascending branch, the FDEMS phase curves first have wide and low amplitude maxima which is followed by the transfer to the right horizontal asymptotes ( $0^\circ$  for  $E_x$  phase). On the  $B_z$  phase curve there is no maxima before right horizontal asymptote at the level of  $90^\circ$ . The amplitude of the vertical magnetic component at the same frequency range has a descending branch, position of which is estimated only by the sounding spacing  $R$ :

$$\rho_a = 1.3 \cdot R \cdot f \quad (8)$$

This asymptote of the nearest zone could be very useful as additional coordinate axis. For the electrical component between the ascending branch and the right asymptote there is a gently sloping maxima, the amplitude of which is closely related to the ratio of the resistivity of second and first layers ( $\rho_2 / \rho_1$ ). The FDEMS curves contain elements closely related to the  $R / h_1$  ratio. Since the sounding spacing  $R$  is always known from the experiment, the FDEMS method can separately determine the values of  $h_1$  and  $S_1$ . Figure 3 shows the key of these elements, based on the ratio of significant points coordinates of the FDEMS curves.

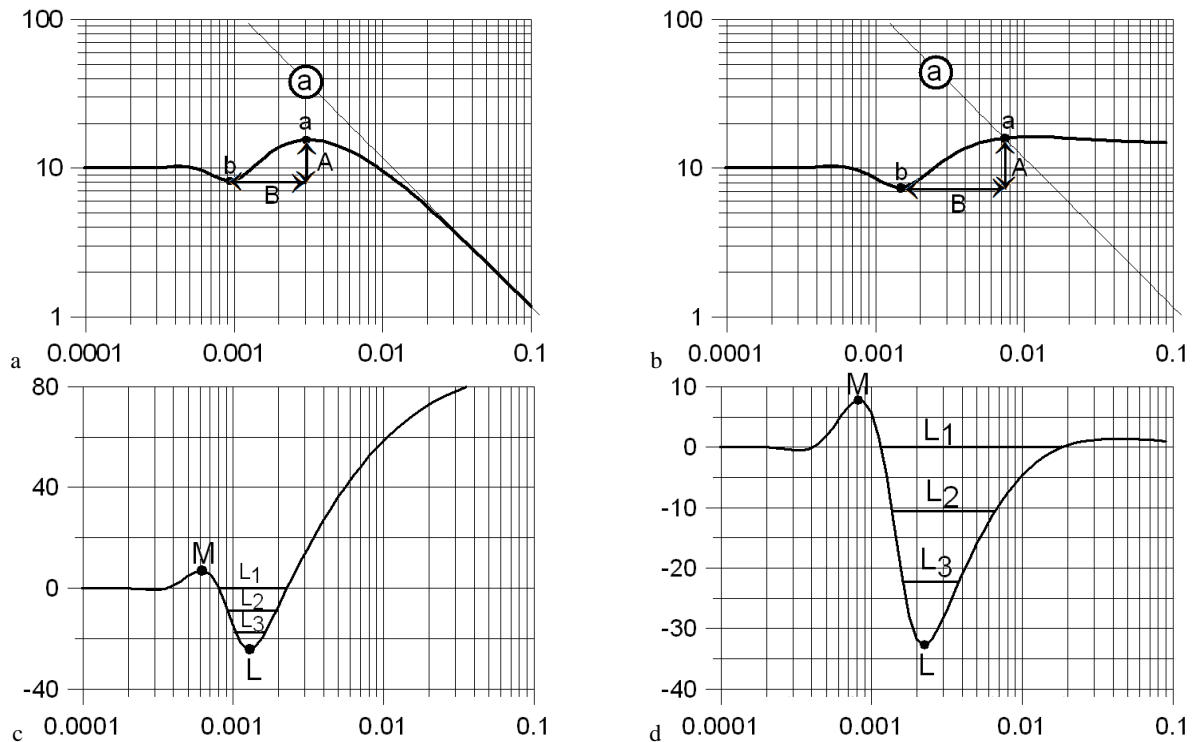


**Figure 3: Significant points of the FDEMS amplitude (a, b) and phase (c, d) curves at the equator of the power dipole:  $\frac{\partial B_z}{\partial \omega}$  (a, c) and  $E_x$  (b, d).**

Parameters marked in the Figure 3 were successfully used for accurate FDEMS data interpretation in various cases (Enestein, 1967, Gorunov et al., 1987, Ingerov et al., 1990, Ingerov and Soldatenko, 1998, Ivanov, 1983, Lozovoy et al., 2011, Shevnin, 1973).

### THE NATURE OF FDEMS CURVES SHAPE AND LEVEL VARIATION WITH ALTERED PARAMETERS OF THE GEOELECTRIC SECTION

Figure 4 shows the FDEMS amplitude and phase curves for the parallel electrical component ( $E_x$ ) over the basic two-layer section and array parameters described in Figure 2 with varying:

- a, b - resistivity of the first layer  $\rho_1$ , whereas the total longitudinal conductivity of the first layer  $S_1$  also changes, while its thickness remains constant ( $h_1 = const$ );
- e, d - thickness of the first layer  $h_1$ , whereas both  $h_1$  and  $S_1$  are varying as well;
- e, f - resistivity of the second layer  $\rho_2$ . In this case only the first and second layers' resistivity ratio varies.

In the first case, as  $\rho_1$  is lowered, the amplitude curves with slight change of their shape move to the right and down. In other words, the left asymptote level changes as well as the asymptote itself and with it changes the wave zone of the source. Phase curves with the decrease of  $\rho_1$  shift to the left along the horizontal axis  $0^\circ$ . However, in this case the ordinate of the minima and the amplitude of the following this minima low maxima are noticeably changing - they are increasing proportionally, whereas the ratio  $\rho_2 / \rho_1$  is decreasing (Figure 4 a, b). The physical meaning of these parameters is clear from Figure 3. As the value of  $\rho_1$  decreases, the ordinate of the interference minima is decreasing in amplitude (Figure 4, e), and the relative value of the maxima following the

ascending branch is increasing as well. The physical cause of this phenomenon is rather clear. With the decrease of  $\rho_2$ , the reflection coefficient  $K$  at the boundary of the first and second layers also decreases (Ingerov et al., 2012, 2015):

$$K = \frac{2(\rho_1 - \rho_2)}{\rho_1 + \rho_2} \quad (9)$$

Accordingly, the amplitude of the reflected wave is attenuated. At the same time, the damping of the refracted wave increases and, as a consequence of these two processes, the interference minima is also attenuated. The same situation is also observed on the phase curves. For  $\rho_2 / \rho_1 > 100$ , the amplitude varies slightly. For multi-layered sections, with a high-resistance reference horizon at the basement, the shape of the graphs may be somewhat different, but the general form will be similar. Thus, in the FDEMS method, it is possible to quickly determine the summed parameters of geoelectrical sections with presence of the high-resistivity reference horizon.

In the second case, not only the level, but also the shape of the curves changes significantly. For the vertical magnetic component, we have two extreme, two characteristic points, which are easily recognizable on the curves. The first of these is the interference minima, and the second is the maxima preceding the curve's transfer to the right asymptote of the near zone. For the electrical component, only the interference minima is confidently recognized, the maxima behind the ascending branch is very low. Therefore, determining its coordinates is a difficult task in the distorted field data curves. It is much more convenient to use as the second significant point the point of intersection of the amplitude curve  $E_x$  with the asymptote of the nearest zone (Equation 8). The ordinate of this point is correlated to the ordinate of the right asymptote by the expression:

$$\rho_{as} = 1.05 \cdot \rho_a \text{ (for } \rho_2 / \rho_1 \geq 100 \text{)} \quad (10)$$

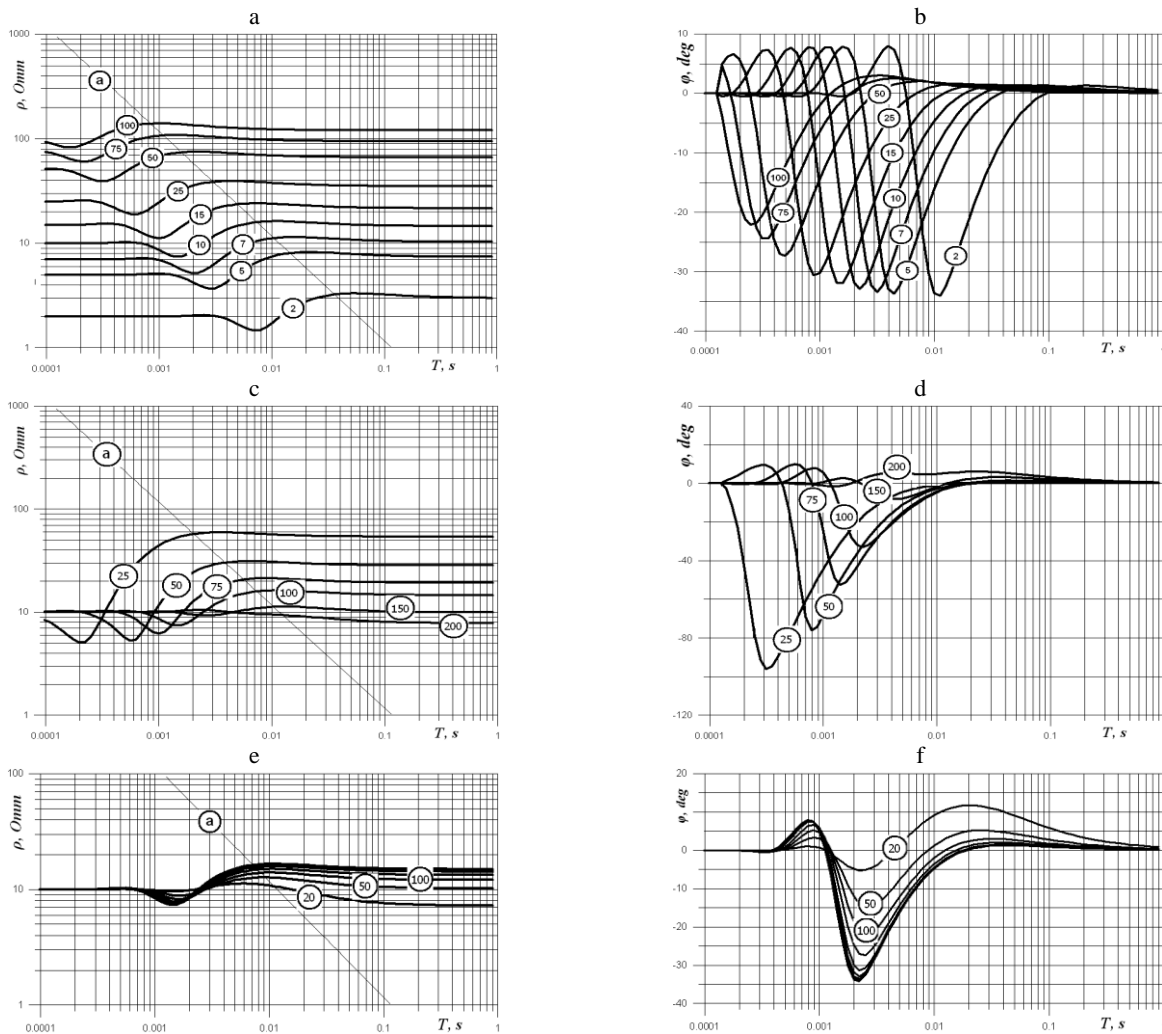


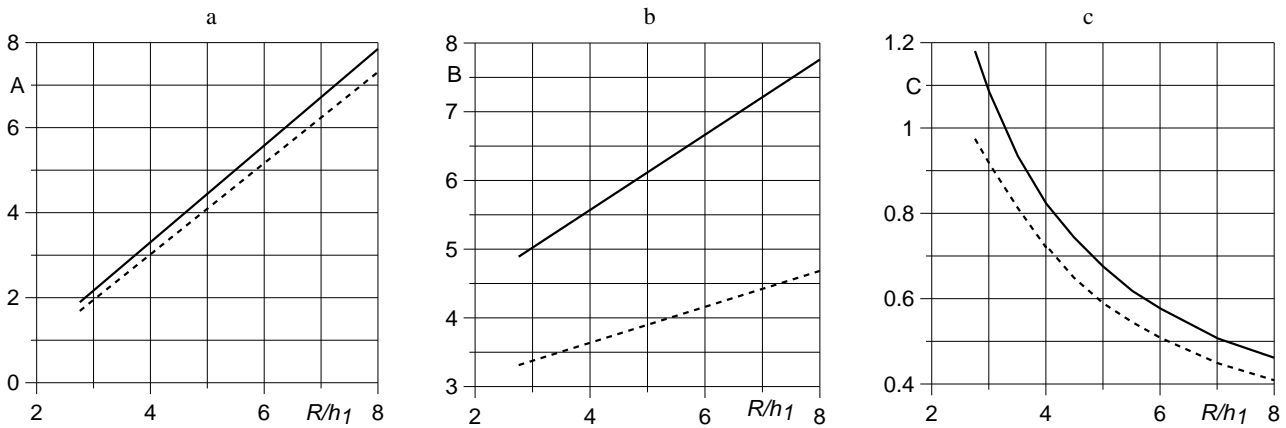
**Figure 4: The FDEMS amplitude (a, c, e) and phase (b, d, f) curves for the  $E_x$  (c, d) component above the two-layer medium with varying: a, b - the resistance of the 1<sup>st</sup> layer; c, d - the thickness of the first layer; e, f - resistance of the 2<sup>nd</sup> layer. Marked in the circles: a - the asymptote of the near zone; numbers - the value of the parameter being changed.**

The parameters associated with the multiplication  $S_1 h_1$  are the abscissas of the amplitude curves ( $S_1 h_1 = k_1 \cdot T_{min}^a / R$ ) and phase curves ( $S_1 h_1 = k_2 \cdot T_{min}^p / R$ ) minima. The parameters associated with the value of  $S_1$  are for  $E_x$  ( $S_1 = R / (2 \cdot \rho_a)$ ) and for  $\frac{\partial B_z}{\partial \omega}$  ( $S_1 = k_{max} \cdot T_{max} / \rho_{min}$ ). The parameters that depend on the ratio  $R / h_1$  for the amplitude curves are  $A = \rho_a / \rho_{min}$  for  $E_x$  and  $A = \rho_{max} / \rho_{min}$  for  $\frac{\partial B_z}{\partial \omega}$ ;  $B = T_a / T_{min}$  for  $E_x$  and  $B = T_{max} / T_{min}$  for  $\frac{\partial B_z}{\partial \omega}$ ;  $C = (\rho_{min} \cdot T_{min}) / R$  for  $E_x$  and  $\frac{\partial B_z}{\partial \omega}$ . For the FDEMS phase curves, it is the ordinate of the minima ( $\Delta \varphi_{min}$ ) and width of the minima at the level  $-10^\circ$  ( $-20^\circ$ ), etc.,  $L_{-10} = -10 T_2 / -10 T_1$  (Figure 3, 4).

Based on the extensive experience of the FDEMS method practical application in the field, the accuracy of determining the summed parameters of the geoelectrical section can be increased to 2-3% of their value (Gorunov et al., 1987, Ingerov and Soldatenko, 1998, Ingerov et al., 2016) using known data as a training sample due to:

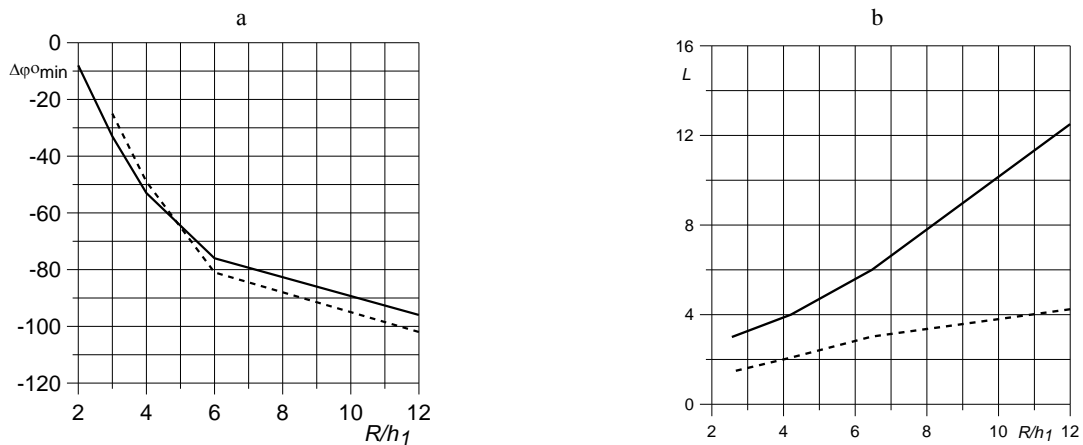
- use of amplitude and phase curves (Gorunov et al., 1987);
- use of finite-difference and normalized finite-difference transformations of the observed curves (Ingerov et al., 2012, 2015);
- use of several array spacings (Ingerov and Soldatenko, 1998);
- complex use in one regression equation of parameters  $A, B, C, S_1, S_1 h_1, \varphi_{min}, L_{1-3}$ , etc. (Ingerov et al., 2016);
- use of several components of the electromagnetic field (Gorunov et al., 1987, Ingerov and Soldatenko, 1998).

Figure 5 shows the graphs of the amplitude curve parameters  $A, B, C$  correlation. Figure 6 shows the phase curves  $\Delta \varphi_{min}$  and  $L_{-10^\circ}$  as the function of the ratio  $R / H$  for a two-layer section with the ratio  $\rho_1 / \rho_2 \geq 100$ .



**Figure 5: Graphs of the dependencies of FDEMS significant points parameters for  $E_x$  (solid line) and  $\frac{\partial B_z}{\partial \omega}$  (dashed line) amplitude curves.**

As can be seen from the Figure 5, these dependencies are convenient to use for determining  $h_1$  in the interval  $3 \leq R / h_1 \leq 8$ . From the economic point of view (the shorter the spacing, the lower are the costs of soundings), this interval is recommended to reduce to  $3 \leq R / h_1 \leq 6$ . According to works of Ingerov et al., (2016), the complex use of these dependencies, similar to the ones shown in Figure 5 and Figure 6, in this regression equation makes it possible to significantly reduce the average error in determining the thickness of  $h_1$  (sedimentary deposits plus weathering crust).



**Figure 6: Graphs of the dependencies of FDEMS significant points as functions of  $R / h_1$  ( $E_x$  - solid line,  $\frac{\partial B_z}{\partial \omega}$  - dashed line) phase curves.**

Thus, in the FDEMS method the interference extreme are much more pronounced than in the magnetotelluric group of methods (Ingerov et al., 2012, 2015). In addition, the amplitude and phase curves present a number of elements closely related to the ratio  $R/h$ . Consequently, in the FDEMS method there is the possibility of robust field data interpretation using the significant points method. Moreover, experience shows (Ingerov et al., 2016) that the accuracy of boundary mapping can be brought to the accuracy of field data. All this opens up encouraging prospects for the effective application of the FDEMS method for carrying out high-precision mapping of boundaries.

## DEVELOPMENT OF HARDWARE AND SOFTWARE FOR THE FDEMS METHOD

In practice, three methods of excitation of the artificial current in the Earth are used:

- *Square wave*, bipolar pulses with successively varying frequencies and application of FFT to determine the amplitude and phase of the fundamental harmonics (a bipolar periodic signal). This technology is most widely warranted itself in the field practice. Both wideband and narrowband recording equipment can be used to register FDEMS signals in the frequency range from 100 000 to 0.01Hz.
- *Square wave with one low frequency* (0.03 or 0.01 Hz). In this case, broadband equipment (up to 10,000 Hz) is used to register the EM field. Signal processing uses signal stacking, followed by the conversion of the recorded data using FFT into frequency amplitude and phase characteristics. Such a technology has been successfully used above sections with high conductivity (more than 500Sm) during oil and gas exploration in Dnipro-Donetsk basin.
- *Harmonic sinusoidal signal*. This mode of operation results in significantly higher load on the motor generator and creates difficulties when working with high currents. This mode is advisable only when working with frequencies 1000 Hz or higher.

### FDEMS field data loggers (receivers)

At the present day, the most suitable and efficient FDEMS equipment is the 8-channel Broadband Multifunction EM GEPARD-8 receiver (generation 5+) with flexible configuration of electrical and magnetic channels. This instrument can accurately and cost-effectively investigate geoelectrical sections in the depth range from 5 to 300m with portable low power current source AT-100 (Ingerov, 2016). The depth of investigation could be increased up to 4000m with more powerful transmitters (30-50kW) (Ingerov, 2011, 2016). One channel portable receiver MARY-24 can also be used in the frequency range 512 – 0.07 Hz (Ingerov, 2011), however field productivity will be significantly lower. Equipment for shallow FDEMS (first few meters) is also manufactured in Novosibirsk, Russia. (Manstein et al., 2008) and is primarily used for geological engineering and archaeological tasks.

### FDEMS Data Processing

FDEMS data processing consists of editing recorded signal from industrial frequency harmonics, impulsive and step noise, decimation, smoothing, transition to the frequency domain and calculation of the amplitude and phase response functions of the medium. Both GEPARD-4/8 and MARY-24 are equipped with corresponding software.

### FDEMS Data Interpretation

- *The method of significant points*. The fundamentals are set out in this article; they have good development prospects for multi-layered sections and are quite effective.
- *Trial and error method*. Effective and easy to use. Experience has shown that within the limits of field data accuracy, the MT amplitude and phase curves were sufficiently approximated by the 7-layer model, whereas minimum 15 layers were required for the FDEMS method for experimental data obtained in Dnipro-Donetsk basin.
- *Inversion*. There is convenient 1-D inversion developed by A. Kaminsky (Zond Software).

Thus, at the moment, the FDEMS method has all the necessary tools of competitively efficient solution for mapping, exploration and geological-engineering problems.

## CONCLUSIONS

- The FDEMS method today has all the attributes of successful geophysical method, serially produced equipment, tested software for field data processing and easily accessible software for 1-D interpretation.
- The FDEMS method due to the effective use of the controlled source's EM field zones, as well as the presence of deep interference extreme, has a significant advantage over other electroprospecting methods in the accuracy of mapping the boundaries of the geoelectrical sections.
- Modern multichannel equipment provides FDEMS method with significant advantages not only in accuracy, but also in productivity and reduced costs of field works over other electroprospecting methods when conducting investigations at depth intervals of 30 - 4000 m.

## ACKNOWLEDGMENTS

Authors acknowledge support and assistance during research provided by Advanced Geophysical Operations and Services Inc. (AGCOS).

## REFERENCES

- Cagniard, L., 1953, Basic theory of the magnetotelluric method of geophysical prospecting: *Geophysics* 18, 605-635.
- Enestein, B.S., 1967, Ways to interpret two-layer frequency sounding curves: *Reports of USSR Academy of Science - Physics of the Earth*, 1967, 9.
- Enestein, B.S., Ivanov, A.P., and Ivanov, M.A., 1961, Equipment for frequency soundings: *Reports of USSR Academy of Science*, Moscow, 1961.
- Gorunov, A.S., Ingerov A.I., and Kulikov A.V., 1987, Equipment EVA-203 application for Frequency Electromagnetic sounding: *Application Geophysics*, 117, 62-69.
- Ingerov, A., 2011, Recent tendencies in onshore and offshore EM equipment development: *Materials of the Fifth all-Russian workshop-seminar in the name of M.N. Berdichevsky and L.L. Vanyan on electromagnetic soundings of the Earth - EMS-2011*, St. Petersburg, Russia, May 16-21, Abstract Book, Vol.1, 86-102.
- Ingerov, A.I., Bugrimov, D.P., Golik, A.I., Pakhomov, S.P., Savchuk, N.A., Seregin, S.B., and Yalansky, A.I., 1990, Combining electromagnetic methods during oil and gas exploration surveys in the Dnipro-Donetsk basin (DDV): *Electromagnetic induction in the upper part of the earth's crust*: Moscow – Nauka, 1990, 156.
- Ingerov, A.I., Bugrimov, D.P., Kipen, I.M., and Savchuk, N.A., 1990, Methodology of frequency domain soundings for mapping the Precambrian crystalline basement on the Ukrainian shield and its slopes: *Electromagnetic induction in the upper part of the earth's crust*: Moscow – Nauka, 1990, 157.
- Ingerov, A.I., Ingerov, I.A., Lozovoy A.L., and Mendriy Y.V., 2012, Application of amplitude and phase curves received by induction sounding with natural sources for the purpose of mapping: *Scientific Bulletin of National Mining University, Scientific and technical journal*, No. 2 (128) 2012, Dnipropetrovsk, Ukraine, 5-10.
- Ingerov, A.I., Ingerov, I.A., Lozovoy A.L., and Mendriy, Ya.V., 2015, Differential curves of induction electromagnetic soundings with natural sources for structural mapping in oil and gas geology: *Scientific Bulletin of National Mining University, Scientific and technical journal*, No. 1, 2015, Dnipropetrovsk, Ukraine, 42-48.
- Ingerov, A.I., and Soldatenko, V.P., 1998, About accuracy of the depth of high resistive reference horizon estimation by methods of frequency electromagnetic sounding: *The reports of National Academy of Science of Ukraine*, 12, 123-128.
- Ingerov, I., 2016, Multifunction 4 and 8 channel electroprospecting instruments of the generation 5+: *Proceedings of the 29th Annual Symposium on the Application of Geophysics to Engineering and Environmental Problems (SAGEEP)*, Denver, Colorado, USA.
- Ingerov, I., Lozoviy, A., Mendrii, Y., 2016, Frequency domain control source EM technology for mineral exploration: *Proceedings of the 29th Annual Symposium on the Application of Geophysics to Engineering and Environmental Problems (SAGEEP)*, Denver, Colorado, USA.
- Ivanov, A.P., 1983, *Frequency Electromagnetic Soundings*: Moscow - Nauka, 1983.
- Kulikov, A.V., and Shemyakin, E.A, 1978, *Electroprospecting by Phase Method of Induced Polarization*: Moscow – Nedra, 1978.
- Lozovoy, A.L., Ingerov, A.I., and Soldatenko, V.P., 2011, The method of significant points FDEMS data interpretation in conditions of Ukrainian Shield: *Materials of the Fifth all-Russian workshop-seminar in the name of M.N. Berdichevsky and L.L. Vanyan on electromagnetic soundings of the Earth - EMS-2011*, St. Petersburg, Russia, May 16-21, Abstract Book, Vol.2, 194-196.
- Manstein, A.K., Panin, G.L., and Tikunov, S.Yu., 2008, A device for shallow frequency-domain electromagnetic induction sounding: *Russian Geology and Geophysics*, 49, 430-436.
- Shevnin, V.A., 1973, Composite nomograms-templates for the interpretation of two-layer frequency sounding curves: *University Reports - Geology and exploration*, 12.
- Tikhonov, A.N., 1950, About determining the electrical properties of deep layers of Earth crust and mantle: *Abstracts of USSR Academy of Science*, series 1950, Vol. 73, 2, 295-297.
- Vanyan, L.L., 1965, *The basis of electromagnetic soundings*: Moscow - Nedra, 1965.